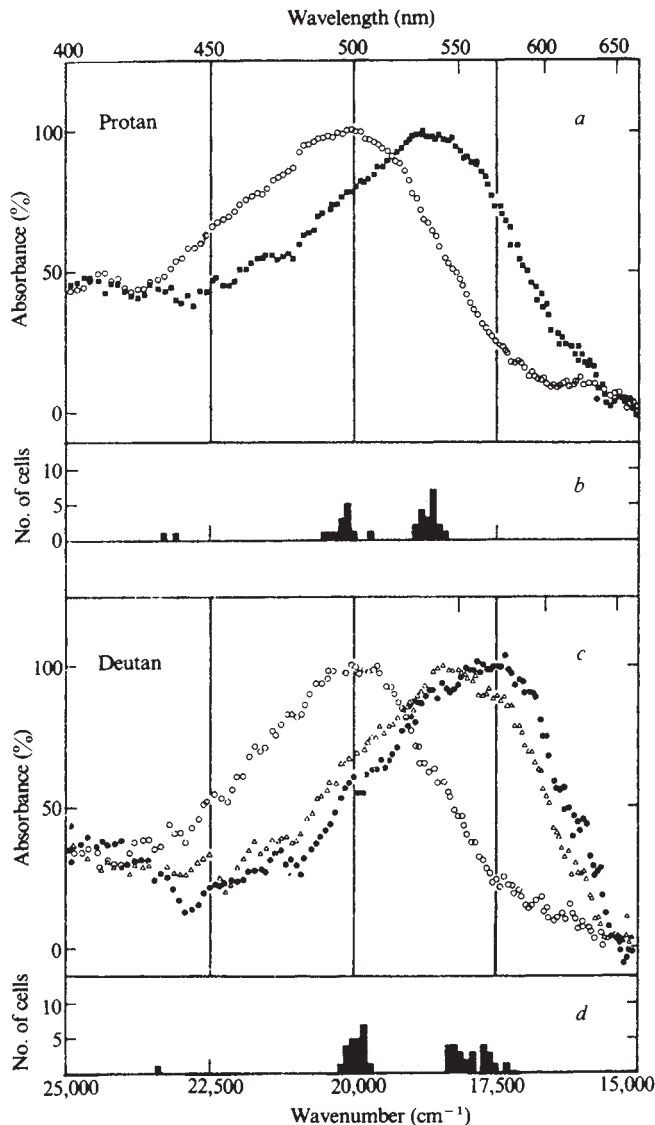


scattering or in the presence of photoproducts at short wavelengths, which would distort the absorbance spectrum.

As in macaques and man<sup>19,20</sup>, the short-wave receptors seem to be rare in squirrel monkeys. In the case of the rods there is a 5-nm difference between animals in  $\lambda_{\max}$ , a difference which is associated with a small difference in absorbance at short wavelengths; we do not know whether the latter difference reflects short-wave contaminants or a true difference in the absorbance spectrum.



**Fig. 3** *a, c*, Mean absorbance spectra for different classes of photoreceptor in two individual squirrel monkeys. Each datum point corresponds to the average of values obtained at two adjacent wavelengths, one value recorded in the descending scan (see text) and the other recorded in the ascending scan. The absorbance spectra for individual receptors were not normalized before averaging. The mean spectra have been normalized to have a maximum of 100%. *b, d*, Distribution of values of peak sensitivity of individual receptors from the protan (*b*) and deutan (*d*) animals. The bin size is  $100\text{ cm}^{-1}$ . With the exception of the three short-wavelength receptors, values of peak sensitivity were derived as follows. The raw absorbance values for individual wavelengths were smoothed using an 11-nm running average. The approximate peak of this curve was estimated and each of 50 individual (smoothed) absorbance values on either side of the provisional peak was referred to an appropriate nomogram to estimate the wavenumber of peak sensitivity; this operation amounts to finding where the nomogram must be located on a wavenumber abscissa to yield the absorbance value under consideration. The mean of the many separate estimates for a given cell is the value entered in the histogram. This method resembles that described by Bowmaker *et al.*<sup>19</sup>, except that the smoothing and subsequent analysis are carried out by the computer and more individual estimates are used. For the three short-wavelength records we estimated wavenumber of peak sensitivity directly from the 2-nm averages (see above) in the restricted range 400–475 nm, using the frog green-rod nomogram<sup>22</sup>.

This first microspectrophotometric study of behaviourally different conspecifics is consistent with classical explanations of colour deficiency and anomaly. Within the limits of our sampling, the severely protan animal lacks entirely the long-wave receptors found in macaques<sup>18,19</sup>. The deuteranomalous animal lacks the P535 receptors found in the protan but probably has more than one type of receptor in the range 546–577 nm.

This work was supported by NIH grant EY-02052 and MRC grant 979/219/N. We thank Professor H. B. Barlow FRS for holding the two independent sets of data, P. F. Martin and B. E. Reese for experimental assistance in Santa Barbara, and Mr M. W. Smith for veterinary supervision in Cambridge.

Received 24 February; accepted 18 June 1981.

1. Boynton, R. M. *Human Color Vision* (Holt, Rinehart & Winston, New York, 1979).
2. Pokorny, J., Smith, V. C., Verriest, G. & Pinckers, A. J. L. G. *Congenital and Acquired Color Vision Defects* (Grune & Stratton, New York, 1979).
3. Voigt, J. H. *Gothaisches Magazin für das Neueste aus der Physik und Naturgeschichte* Vol. 1 (ed. Lichtenberg, L. C.) 57–61 (Ettinger, 1781).
4. Palmer, G. *Théorie de la Lumière, Applicable aux Arts et Principalement à la Peinture* (Hardouin & Gattey, Paris, 1786).
5. Walls, G. L. *J. hist. Med.* **11**, 66–96 (1956).
6. Rayleigh, Lord *Nature* **25**, 64–66 (1881).
7. von Kries, J. in *Handbook of Physiological Optics* Vol. 2 (von Helmholtz, H.) (translated by Southall, J. P. C.) (Optical Society of America, 1924).
8. Hurvich, L. M. & Jameson, D. *Documenta Ophth.* **16**, 409–442 (1962).
9. Alpern, M. & Torii, S. *J. gen. Physiol.* **52**, 717–737, 738–749 (1968).
10. Rushton, W. A. H., Powell, D. S. & White, K. D. *Vision Res.* **13**, 2017–2031 (1973).
11. MacLeod, D. I. A. & Hayhoe, M. J. *opt. Soc. Am.* **64**, 92–96 (1974).
12. Jacobs, G. H. *Science* **197**, 499–500 (1977).
13. Jacobs, G. H. & Blakeslee, B. *Invest. Ophth. vis. Sci. Suppl.* **136** (1980).
14. Marks, W. B., Dobelle, W. H. & MacNichol, E. F. *Science* **143**, 1181–1183 (1964).
15. Brown, P. K. & Wald, G. *Science* **144**, 45–51 (1964).
16. Liebman, P. A. & Entine, G. J. *opt. Soc. Am.* **54**, 1451–1459 (1964).
17. Dobelle, W. H., Marks, W. B. & MacNichol, E. F. *Science* **166**, 1508–1510 (1969).
18. Bowmaker, J. K., Dartnall, H. J. A., Lythgoe, J. N. & Mollon, J. D. *J. Physiol., Lond.* **274**, 329–348.
19. Bowmaker, J. K., Dartnall, H. J. A. & Mollon, J. D. *J. Physiol., Lond.* **298**, 131–143 (1980).
20. Bowmaker, J. K. & Dartnall, H. J. A. *J. Physiol., Lond.* **298**, 501–511 (1980).
21. Cooper, R. W. in *The Squirrel Monkey* (eds Rosenblum, L. A. & Cooper, R. W.) 1–29 (Academic, New York, 1968).
22. Knowles, A. & Dartnall, H. J. A. *The Photobiology of Vision* (Academic, New York, 1977).

## Spatial summation and contrast sensitivity of X and Y cells in the lateral geniculate nucleus of the macaque

Robert Shapley, Ehud Kaplan & Robert Soodak

The Rockefeller University, 1230 York Avenue, New York, New York 10021, USA

Study of parallel processing in the visual pathway<sup>1</sup> of the cat has revealed several classes of retinal ganglion cells which are physiologically distinct and which project to various locations in the brain<sup>2,3</sup>. Two classes have been studied most extensively: X cells, which sum neural signals linearly over their receptive fields, and Y cells, in which the spatial summation is nonlinear<sup>1,4</sup>. In the cat's lateral geniculate nucleus (LGN) cells also can be classified as X or Y, a result of the parallel projection of retinal X and Y inputs to different geniculate neurones<sup>5–9</sup>. We report here our study of parallel signal processing in the LGN of the macaque monkey. We find that (1) monkey LGN cells can be classified as X or Y on the basis of spatial summation; (2) X-like cells are found in the four parvocellular and the two magnocellular laminae, whereas Y-like cells are found almost exclusively in the magnocellular laminae; and (3) the cells of the magnocellular laminae have high sensitivity and the parvocellular cells low sensitivity for homochromatic patterns. This implies that in macaque monkeys the magnocellular cells and their cortical projections may be the neural vehicle for contrast vision near threshold. The cells of the parvocellular laminae seem to be primarily concerned with wavelength discrimination and patterns of colour. As the human visual system is similar to that of the macaque in structure and behavioural performance, our findings are probably also applicable to man.

In macaque monkeys, as in man, the LGN is a highly organized, layered nucleus. There are four dorsal layers of small

cells (parvocellular) and two ventral layers of large cells (magnocellular). Previous investigators<sup>10-12</sup> concluded that there was a complete segregation of X and Y cells in the monkey's geniculate nucleus, the X cells residing in the parvocellular laminae and the Y cells in the magnocellular laminae. These conclusions depended on identifying X and Y cells by the time course of response to visual stimulation and the latency of response to electrical stimulation of the optic chiasm. Although such characteristics have been used to classify X and Y cells in the cat LGN<sup>6,7</sup>, a correlation between response time course and linearity of spatial summation has not been established for neurones of the monkey's LGN.

In our experiments we used nine cynomolgus monkeys (*Macaca fascicularis*) anaesthetized with urethane (20 mg per kg per h) and paralysed with Flaxedil. The activity of single cells was recorded extracellularly using glass micropipettes (tip resistance, 10–30 M $\Omega$ ). In about half the penetrations the pipettes were filled with a saturated solution of Fast Green dye in Ringer's solution to mark the position of the recording electrode. Electrode tracks were reconstructed from histological sections by using the dye marks and distances traversed along the track. This was important for assigning a given cell to a particular geniculate lamina because laminar boundaries are often irregular and the layer 3–layer 2 boundary, which is the critical parvocellular–magnocellular boundary, is not accompanied by an eye change. Visual stimuli were produced electronically on the face of a CRT<sup>13</sup> which subtended 10° by 8° in

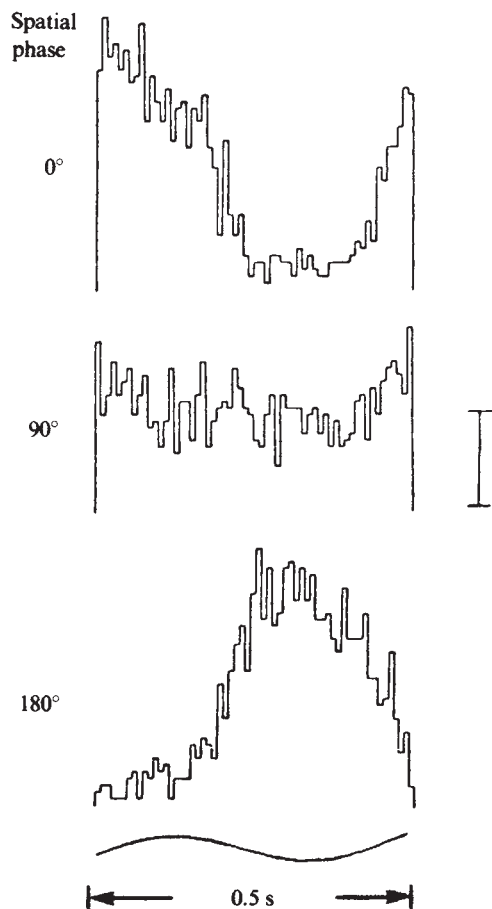


**Fig. 1** Response of an X cell from a magnocellular layer at three different positions (spatial phases). The cell was recorded in layer 2 of the macaque's LGN. The stimulus was a sine grating of 1.5 cycle deg<sup>-1</sup>, 50% contrast, contrast reversed with a sinusoidal time course at 2 Hz as indicated at the bottom of the figure. 0° and 180° were spatial phases at which the stimulus produced maximal responses; 90° was the spatial phase of the null response. The vertical calibration, drawn close to the middle histogram, is 30 impulses per second.

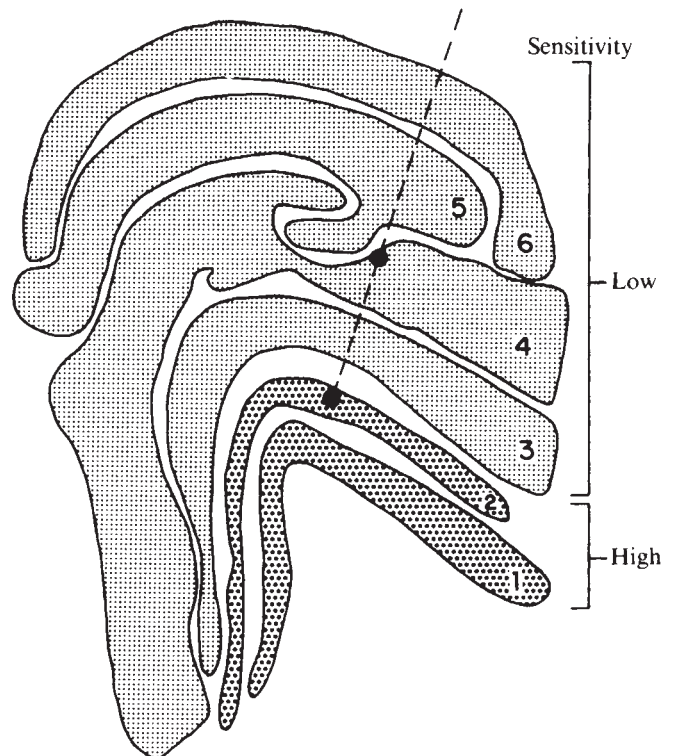


**Fig. 2** Contrast sensitivity in the macaque's LGN. This drawing is traced from a single 100- $\mu$ m thick section of the LGN. The parvocellular laminae are numbered 6, 5, 4 and 3 and the magnocellular laminae 2 and 1. The parvocellular cells all had lower contrast sensitivity than did the X and Y cells of the magnocellular laminae. A reconstructed electrode track is shown; the two dark circles represent green dots left by the electrode at sites where (1) a typical parvocellular X cell of low sensitivity was recorded in layer 4 and (2) a typical magnocellular X cell of high contrast sensitivity (>50) was recorded in layer 2. The latter was the first cell of high contrast sensitivity found on this track.

visual angle. In some experiments a CRT with a P31 (green) phosphor was used, in others a CRT with a P4 (white) phosphor with no difference in results. The mean luminance was 20–60 cd m<sup>-2</sup>, in the low photopic range. The pupils were dilated to ~6-mm diameter and the eyes protected with clear plastic contact lenses. In several experiments Wratten colour filters (no. 26, red; no. 61, green; no. 48A, blue) were placed in front of the CRT to check whether linearity of spatial summation depended on the colour of the screen.

Cells were classified as X or Y by means of their response to sine gratings, patterns in which the luminance varied sinusoidally with position in one dimension. The contrast of the gratings was reversed with a sinusoidal time course<sup>4,8,9</sup>. A cell was called X if it responded to low and high spatial frequency patterns as if it received input from a single linear receptive field mechanism. This means that an X cell would respond to contrast reversal of the grating at the temporal modulation frequency, and its response would exhibit a sinusoidal dependence on the position (or spatial phase) of the grating<sup>4,8,9</sup>. A cell was called Y if it responded to low spatial frequencies approximately like an X cell, but revealed only nonlinear behaviour at higher spatial frequencies. The nonlinear behaviour looked for, based on our experience with cat Y cells, was frequency doubling of responses to contrast reversal. In monkey Y cells, as in the cat, a frequency-doubled response was present at all positions of the grating. Classification of cells as X or Y did not depend on the colour of the screen in the experiments with Wratten filters. That retinal ganglion cells in the monkey can be classified as X or Y has been previously reported<sup>14</sup>. Thus, in the monkey, as in the cat, retinal ganglion cells confer their characteristic properties on their geniculate targets.



Cells classified as X by above criterion were found in all laminae of the macaque's LGN. Figure 1 shows the responses of a magnocellular X cell to the stimulus of a 1.5 cycle  $\text{deg}^{-1}$  sine grating undergoing contrast reversal with a sinusoidal time course at 2 Hz. Responses at three different positions or spatial phases are shown: at  $0^\circ$  spatial phase there was a maximal response, at  $90^\circ$  no response, and at  $180^\circ$  the response peaked again.

Almost all the parvocellular cells recorded were X cells (225 out of 226 cells recorded and assigned to the parvocellular laminae by histological reconstruction of tracks); only one was a Y cell. Most of the magnocellular cells recorded were also X cells (59 out of 77 cells assigned to the magnocellular layers); the rest were Y cells. Thus, our results show that magnocellular cells do not form a homogeneous class with respect to spatial summation properties. Similar results have been reported in preliminary form elsewhere<sup>15-18</sup>.

We next investigated functional differences between parvocellular and magnocellular cells by comparing their contrast sensitivities. Contrast sensitivity was determined as the reciprocal of the contrast required to give a modulated discharge with an amplitude of 5 impulses per second in response to a drifting sine grating. The spatial frequency of the grating was varied from 0 to 10 cycle  $\text{deg}^{-1}$ , and the peak contrast sensitivity for each cell was determined. The parvocellular cells had much lower peak contrast sensitivity than the magnocellular cells. The parvocellular cells had a peak contrast sensitivity of 10. Both X and Y cells in the magnocellular laminae had a peak contrast sensitivity of approximately 75. The contrast sensitivity of magnocellular cells was high enough that it might account for the behavioural contrast sensitivity of *Macaca fascicularis*<sup>19</sup>. Figure 2 shows that the magnocellular layers are the site of high contrast sensitivity and the parvocellular laminae contain cells which are relatively insensitive to luminance contrast. Our discovery that parvocellular neurones have low contrast sensitivity is consistent with previous evidence that these cells analyse colour<sup>10,12,20,21</sup>. Note that peak contrast sensitivity did not show a strong dependence on the colour of the CRT screen in the experiments with Wratten filters.

The contrast sensitivities of cells in the magnocellular laminae of the monkey are comparable with those of cells in the A and A1 laminae of the cat LGN. As the parvocellular X cells were far less sensitive to contrast, the proposed homology between the X cells in the parvocellular laminae of the monkey and X cells in the cat LGN<sup>10-12</sup> is not compelling. A closer homology exists between the X and Y cells of the magnocellular laminae and the X and Y cells of the cat LGN. The parvocellular laminae of the monkey's LGN, and their retinal inputs, seem to form a visual neural pathway which is not present in cats.

This work was supported by grants EY1472, EY188 and EY1428 from the US NIH. R.M.S. was supported by a Career Development Award and E.K. was partially supported by a NIH Academic Investigator Award and by a grant from Fight for Sight Inc.

Received 8 April; accepted 25 June 1981.

- Enroth-Cugell, C. & Robson, J. G. *J. Physiol., Lond.* **187**, 517-552 (1966).
- Rodick, R. W. A. *Rev. Neurosci.* **2**, 193-225 (1979).
- Lennie, P. *Vision Res.* **20**, 561-594 (1980).
- Hochstein, S. & Shapley, R. M. *J. Physiol., Lond.* **262**, 237-264 (1976).
- Shapley, R. M. & Hochstein, S. *Nature* **256**, 411-413 (1975).
- Cleland, B. G., Dubin, M. W. & Levick, W. R. *J. Physiol., Lond.* **217**, 473-496 (1971).
- Hoffmann, K. P., Stone, J. & Sherman, S. M. *J. Neurophysiol.* **35**, 518-51 (1972).
- So, Y. T. & Shapley, R. M. *Expl Brain Res.* **36**, 535-550 (1979).
- So, Y. T. & Shapley, R. M. *J. Neurophysiol.* **45**, 107-120 (1981).
- Dreher, B., Fukada, Y. & Rodick, R. W. *J. Physiol., Lond.* **258**, 433-452 (1976).
- Sherman, S. M., Wilson, J. R., Kaas, J. H. & Webb, S. V. *Science* **192**, 475-477 (1976).
- Schiller, P. H. & Malpeli, J. G. *J. Neurophysiol.* **41**, 788-797 (1978).
- Shapley, R. M. & Rossetto, M. *Behav. Res. Meth. Instrum.* **8**, 15-20 (1976).
- De Monasterio, F. *J. Neurophysiol.* **41**, 1394-1417 (1978).
- Kaplan, E. & Shapley, R. M. *Invest. Ophthalmol. vis. Sci. suppl.* **19**, 41 (1980).
- Shapley, R. M. & Kaplan, E. *Neurosci. Abstr.* **6**, 583 (1980).
- Blakemore, C. B. & Vital-Durand, R. *Trans. ophthalmol. Soc. U.K.* **99**, 363-368 (1980).
- Lennie, P. & Derrington, A. M. *Invest. Ophthalmol. vis. Sci. suppl.* **20**, 14 (1981).
- DeValois, R., Morgan, H. & Snodderly, D. M. *Vision Res.* **14**, 75-81 (1974).
- Wiesel, T. & Hubel, D. H. *J. Neurophysiol.* **29**, 1115-1156 (1966).
- DeValois, R. & DeValois, K. in *Handbook of Perception* Vol. 5, 116-168 (1975).

## Two genes interact to control development of a lymphoid/erythroid hyperplastic disorder of mice

Luisa DeGiorgi, Arpi Matossian-Rogers & Hilliard Festenstein

Department of Immunology, London Hospital Medical College, Turner Street, London E1 2AD, UK

We have previously established the presence of a gene in mice (called *Lus*)<sup>1</sup> which is dominant for the suppression of cytostasis, an experimental assay of cell-mediated immunity<sup>2</sup>. Here we describe the definition of a gene (segregating independently of *Lus*) that, in combination with the dominant gene *Lus*<sup>a</sup>, is homozygous recessive for a lymphoid hyperplastic disorder of T and B cells. We have called this gene *Arp*. The disease involves abnormalities of lymphopoietic and other organs, and could be a model system for regulatory defects of the immune system.

'Cytostasis' is an *in vivo/in vitro* assay of cell-mediated immunity<sup>3</sup>. In our experiments mice were sensitized by injections of allogeneic lymphoid cells<sup>4</sup>. After 14 days we tested lymph node cells from sensitized mice in an *in vitro* cytostasis assay, using tumour cells as target cells.

Cytostasis is assayed by the uptake of radioactive thymidine by the tumour cells and is positive if uptake is inhibited by the effector cells. Both T and B cells (A. M.-R., L. DeG. and H. F., in preparation) are capable of causing cytostasis. Allogeneic cytostasis following sensitization across the H-2 barrier usually gives a positive result. However, we noted that whereas immunization of CBA/H (H-2<sup>k</sup>) mice with BALB/c spleen cells led to the production of cytostatic effectors against SL2 (H-2<sup>d</sup>) tumour cells (a spontaneous Thy-1-positive DBA/2 lymphoma), immunization with B10.D2 (also H-2<sup>d</sup>) spleen cells failed to generate anti-H-2<sup>d</sup> effectors in the CBA/H (H-2<sup>k</sup>) recipients. Mating B10.D2 with BALB/c mice produced F<sub>1</sub> hybrids whose spleen cells also did not stimulate the production of cytostatic effector cells, suggesting the presence of a dominant suppressor gene in the B10.D2 mice. This finding was further studied and confirmed using (B10.D2 × BALB/c)F<sub>1</sub> × BALB/c backcross mice up to the fourth generation<sup>2</sup> and beyond. Approximately 50% of backcross mice from each generation failed to stimulate the production of cytostatic effectors and were therefore carrying the cytostasis suppressor gene *Lus*<sup>a</sup> (ref. 1 and Tables 1, 2). These were selected for further backcrossing to BALB/c, to develop a strain congenic with BALB/c at the suppressor locus. This was done up to the tenth generation backcross.

After the fourth backcross mating, we first noted the appearance of the hyperplastic disorder with abnormalities in the lymphopoietic and other organs in ~50% of 3-4-week old mice carrying the suppressor gene (Table 2), that is, cytostasis-negative mice. The disorder was manifested by gross hyperplasia of the thymus, spleen (Fig. 1), Peyer's patches and lymph nodes. There were concomitant histopathological changes in these

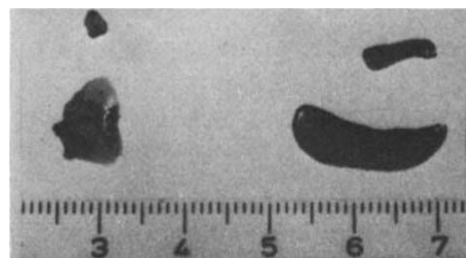


Fig. 1 Spleen and thymus from hyperplastic (right) and non-hyperplastic (left) cytostasis-negative littermates. Note the approximate 10-fold difference between the size of the organs.